doi:10.1016/j.jmb.2004.11.014 J. Mol. Biol. (2005) 345, 1071–1081

JMB

Available online at www.sciencedirect.com

SCIENCE DIRECT®

ELSEVIER

Conferring the Binding Properties of the Mouse MHC Class I-related Receptor, FcRn, onto the Human Ortholog by Sequential Rounds of Site-directed Mutagenesis

Jinchun Zhou[1], Fernando Mateos[1], Raimund J. Ober[1,2] and E. Sally Ward[1,3]*

[1]*Center for Immunology University of Texas Southwestern Medical Center 6000 Harry Hines Blvd., Dallas TX 75390-9093, USA*

[2]*Department of Electrical Engineering, University of Texas at Dallas, Richardson TX 75080, USA*

[3]*Cancer Immunobiology Center University of Texas Southwestern Medical Center 6000 Harry Hines Blvd., Dallas TX 75390-9093, USA*

**Corresponding author*

The MHC class I-related receptor, FcRn, is involved in binding and transporting immunoglobulin G (IgG) within and across cells. In contrast to mouse FcRn, which binds to IgGs from multiple different species, human FcRn is surprisingly stringent in binding specificity. For example, human FcRn does not bind to mouse IgG1 or IgG2a and interacts only weakly with mouse IgG2b. Here, we have used site-directed mutagenesis in combination with interaction (surface plasmon resonance) studies, with the goal of generating human FcRn variants that more closely resemble mouse FcRn in binding specificity. Our studies show that residues encompassing and extending away from the interaction site on the α2 helix of FcRn play a significant and most likely indirect role in FcRn–IgG interactions. Further, by combining mutations in the α2 helix with those in a non-conserved region of the α1 helix encompassing residues 79–89, we have generated a human FcRn variant that has properties very similar to those of mouse FcRn. These studies define the molecular basis for the marked difference in binding specificity between human and rodent FcRn, and give insight into how human FcRn recognizes IgGs.

Keywords: affinity; neonatal Fc receptor, FcRn; pH dependence; site-directed mutagenesis; surface plasmon resonance

Introduction

The MHC class I-related receptor, FcRn, appears to play a general role in regulating the immunoglobulin G (IgG) levels throughout the body.[1] For example, through its ability to bind and transport IgG, FcRn delivers this ligand across epithelial and endothelial barriers *via* transcytosis, in addition to functioning as a recycling receptor.[2–7] Recent data demonstrate that the interaction of IgGs with FcRn following uptake into cells results in sorting away from lysosomal degradation and subsequent exocytosis.[8,9] In contrast, IgGs that do not bind enter the lysosomal pathway. This provides a mechanism by which FcRn maintains relatively constant serum IgG levels.[10–12] Although the majority of studies of FcRn function have been carried out in rodents, the isolation of a human ortholog of rodent FcRn[13] together with functional studies indicate that the roles of FcRn across mammalian species are similar.[1]

Despite the similarity in function for FcRn across species, in an earlier study we reported that whilst mouse FcRn binds to IgGs from a wide range of sources, human FcRn shows a high degree of selectivity in binding and only interacts with a limited subset of the IgGs analyzed.[14] Significantly, relative to mouse FcRn the affinities of human FcRn for mouse IgGs are immeasurably low (with the exception of mouse IgG2b for which weak binding is observed). Here, we have used site-directed mutagenesis and interaction analyses to gain insight into the molecular basis for this variation in specificity across species. Understanding the basis of this marked difference is of practical relevance as it impinges on the validity of the use

Abbreviations used: IgG, immunoglobulin G; SPR, surface plasmon resonance; PBS, phosphate-buffered saline.

E-mail address of the corresponding author: sally.ward@utsouthwestern.edu

of mice as a model for human FcRn. Knowledge as to how human FcRn interacts with cognate IgGs at the molecular level also has relevance to the engineering of antibodies for therapy.

The interaction of both human and rodent FcRn with IgG ligand has been studied at the molecular level.[15–19] Binding of FcRn to IgG involves a site on IgG that encompasses several well-conserved residues at the CH2–CH3 domain interface.[15–22] These residues include the highly conserved amino acid residues Ile253, His310 and His435. Additional binding specificity is contributed by a less well conserved residue at position 436 (His436 in rodent IgGs with the exception of mouse IgG2b; Tyr436 in human IgG1, IgG2, IgG4 and mouse IgG2b).[16,18,21,22] From the X-ray crystallographic structure of rat Fc complexed with rat FcRn,[21] the key FcRn and IgG residues for the rat receptor–ligand interaction have been mapped and are consistent with functional studies.[15–19,22] Significantly, the X-ray structure[21] also demonstrates interactions between acidic FcRn residues and IgG histidine residues that mediate the pH dependence of the FcRn–IgG interaction (strong binding at pH 6.0 that becomes progressively weaker as pH 7.3 is approached).[22,23]

Despite similarities in the residues that constitute the FcRn–IgG interaction site across species, a noticeable difference is a non-conservative change of Asp137 of rat FcRn (or Glu137 in mouse FcRn) to Leu137 in human FcRn.[13,24] In the rat FcRn–IgG structure, Asp137 interacts with His436 of IgG.[21] Using site-directed mutagenesis we recently demonstrated that the amino acid difference at position 137 of FcRn could account, in part at least, for the difference in binding specificity of human *versus* mouse FcRn.[25] We hypothesized that the ability of a human FcRn variant with glutamic acid at residue 137 (L137E) to bind to mouse IgGs was due to an unfavorable Leu137 (FcRn)-His436 (IgG) interaction being replaced by a more favorable Glu137-His436 pair. However, the affinities of this L137E variant for binding to mouse IgGs were about 20-fold lower than the corresponding mouse FcRn–IgG interactions[25] and the molecular basis for these observations was not understood. Here, the goal is to address this issue.

We have analyzed the effects of mutating human FcRn residues that are in the vicinity of key binding residues such as amino acid residue 137 on the interactions with mouse IgGs and human IgG1. The majority of the targeted amino acid residues would be predicted to not make direct contact with IgG ligand.[21] This approach has allowed us to delineate the molecular basis of the distinct binding specificities of mouse and human FcRn. We show that residues in the α2 helix extending away from residue 137 (Leu or Glu) play an important role in FcRn–IgG interactions. FcRn–IgG binding is further modulated by amino acid residues 79–89 in the α1 helix that are spatially close to residue 137 and also contain a potential *N*-linked glycosylation site at residue 87 that is present in rodent but not human FcRn.[13,24,26] Our analyses have relevance to understanding the molecular basis of the high binding specificity that is a characteristic feature of human FcRn.

Results

Rationale for the generation of the mutated derivatives of human FcRn

Here, the goal was to identify the amino acid residues that are responsible for the marked difference in binding specificity between human and mouse FcRn. An alignment of the sequences of human, mouse and rat FcRn with sequence differences indicated (note that we have ignored the two residue deletion of human FcRn to facilitate comparison of rodent and human FcRn sequences[13,24,26]) is shown in Figure 1 of the Supplementary Material. In an earlier study we showed that mutation of Leu137 of human FcRn to the corresponding mouse residue (Glu; L137E mutation) resulted in a human FcRn species that binds to mouse IgG1 and mouse IgG2b with equilibrium dissociation constants of 13.2 μM and 11.7 μM, respectively.[25] From the X-ray crystallographic structure of rat FcRn complexed with rat Fc,[21] residue 137 of FcRn contacts residue 436 of IgG (Table 1 of the Supplementary Material; and Figure 1), and the effect of mutating Leu137 to Glu137 is therefore predicted to be due to more favorable Glu (FcRn)-His (mouse IgG1) interactions. However, the affinities of the L137E mutant for binding to mouse IgG1 and mouse IgG2b were substantially lower than those for the corresponding mouse FcRn interactions.[25]

Here, we have probed additional regions of FcRn that might modulate binding. Specifically, the residues that flank amino acid residue 137 and extend away from the interaction site along the α2 helix of FcRn have been mutated (Figures 1 and 2). These mutations have been combined with alterations of α1 helix residues 79-89 of human FcRn. Mutated proteins (Figure 2) have been expressed, purified and used in surface plasmon resonance (SPR) studies with mouse IgG1, mouse IgG2b and human IgG1, which differ in several residues at the putative FcRn–IgG interaction site (Table 1 of the Supplementary Material).

The FcRn–IgG interaction involves two possible sites on IgG that are not equivalent,[27,28] most likely due to steric effects of occupancy of the first site partially blocking the second site.[29] To avoid avidity effects during SPR analyses, all affinities were determined with IgG immobilized and FcRn in solution. In earlier studies[25] where, in general, the FcRn–IgG interactions were of lower affinity than here, the analyte (FcRn) concentrations used were such that the major contribution to the interactions came from the higher-affinity binding sites on IgGs. This was consistent with the linearity of the Scatchard plots, suggesting a

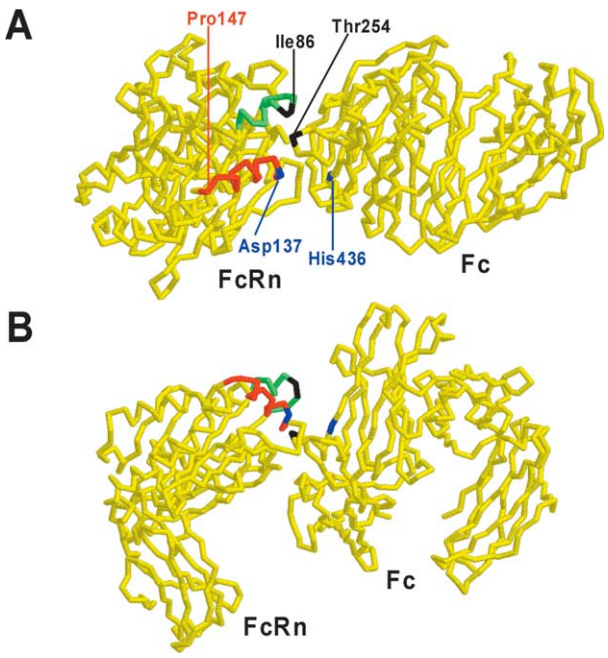

Figure 1. The α-carbon trace of rat FcRn bound to rat Fc[21] (IgG2a derived) with regions that were mutated here indicated. Ile86 (black) and Asp137 (blue) of rat FcRn interact with Thr254 (black) and His436 (blue) of rat Fc, respectively. A, The "top" view of FcRn, to display the two α helices that flank a narrow groove. B, An approximate 90° rotation of the structure in A to show the side view of FcRn. Other residues that play a role in the rat FcRn–rat Fc interaction are not shown, but are fully described by Martin *et al*.[21] Residues 85 and 86 (black) are deleted in human FcRn (Figure 1 of the Supplementary Material). Mouse FcRn residues 79–89 and 136–147 are very similar in rat FcRn (shown in green and red, respectively) and were used to replace the corresponding sequences in human FcRn. The Figure was drawn using RASMOL (Roger Sayle, Bioinformatics Research Institute, University of Edinburgh, Edinburgh, UK).

monophasic 1:1 interaction.[25] Here, for interactions with $K_D > \sim 2.8$ μM, the data were fitted adequately by a 1:1 interaction model (indicated by only one K_D value in Table 1). However, the majority of affinities are higher than those described,[25] resulting in significant levels of occupancy of the "second" lower-affinity sites on IgGs and non-linearity of Scatchards. These data were therefore fitted to a more complex interaction model (two-site negative cooperativity model; see Methods) in which two dissociation constants (K_{D1} and K_{D2}) were estimated.

Analyses of the effects of mutating residues 136–147 of human FcRn

Mutation of residues 136–147 of human FcRn to those of mouse FcRn (136-147) generated a human FcRn variant that has similar dissociation constants for binding to mouse IgG1 as those corresponding to mouse FcRn (Figures 3 and 4, and Table 1). In contrast, the dissociation constants for mouse IgG2b and human IgG1 are about fivefold to 30-fold higher. As human IgG1 and mouse IgG2b both have tyrosine at position 436 (whereas mouse IgG1 has histidine at this location), and residue 436 of rat Fc interacts with Asp137 of rat FcRn,[21] we also made a mutant comprising 136–147 with leucine at position 137 (136-147/L137). This generated a variant with decreased dissociation constants (K_{D1}s) for the Tyr436-containing antibodies, human IgG1 and mouse IgG2b, that were closer to those corresponding to mouse FcRn (Figures 3 and 4, and Table 1). However, relative to mouse FcRn the 136-147/L137 mutant had approximately four- to sixfold higher dissociation constants for mouse IgG1. Nevertheless, the affinities of the 136-147 and 136-147/L137 mutants for mouse IgGs were all substantially increased relative to those of the L137E mutant (Table 1 and the work done by Zhou *et al*.[25]), indicating that residues extending away from the putative binding interface (Figure 1) can increase the interaction strength through longer-range effects.

We also probed the role of the region encompassing residues 136–147 of FcRn in ligand binding by carrying out a reciprocal mutation, i.e. mutating residues 136–147 of mouse FcRn to the corresponding human FcRn sequence. The resulting mutant binds to mouse IgG1 with an immeasurably low affinity. The dissociation constants (K_{D1}s; K_{D2}s were too high to estimate) for binding to mouse IgG2b and human IgG1 are 20.5 μM and 7.4 μM, respectively. This mutated mouse FcRn therefore resembles wild-type human FcRn, although the affinity for binding to human IgG1 is markedly weaker (Table 1). These data reinforce the importance of amino acid residues 136–147 of FcRn in determining binding specificity.

We next attempted to delineate the amino acid residues within residues 136–147 that might be responsible for the improvements in affinities of the human FcRn mutants. This was done by truncating the 136-147 mutation into two en-bloc alterations of 136-142 and 143-147. The 143-147 mutation was also combined with L137E (L137E/143-147), as the L137E change is central to broadening the binding specificity of human FcRn.[25] In addition, two 136-142 mutations were made with Glu (mouse FcRn) and Leu (human FcRn) at position 137 (136-142 and 136-142/L137, respectively). The effects of these mutations on binding are shown in Table 1. From these results it is clear that whilst the 136-142 and 136-142/L137 mutations result in marked improvements in binding affinities for mouse IgG1 and mouse IgG2b relative to wild-type human FcRn, the dissociation constants are, in general, higher than those for the corresponding 136-147 and 136-147/L137 mutations. More dramatic losses in affinity are observed for the L137E/143-147 mutant, and this human FcRn variant has properties that are very similar to those of the L137E mutant (Table 1). In addition,

```
Human FcRn           79   FKALGG--KGPYTLQGLLGCELGPDNTSVPTAKFALNGEE  118
Mouse FcRn           79   L.T.EKILN.T..........AS..S.....V.......  118
136-147              79   ......--..............................  118
136-147/L137         79   ......--..............................  118
136-142              79   ......--..............................  118
136-142/L137         79   ......--..............................  118
143-147              79   ......--..............................  118
L137E/143-147        79   ......--..............................  118
79-89/136-147        79   L.T.EKILN.T...........................  118
79-89/136-147/L137   79   L.T.EKILN.T...........................  118

Human FcRn           119  FMNFDLKQGTWGGDWPEALAISQRWQQQD  147
Mouse FcRn           119  ..K.NPRI.N.T.E...TEIVANL.MK.P  147
136-147              119  ................TEIVANL.MK.P  147
136-147/L137         119  ................T.IVANL.MK.P  147
136-142              119  ................TEIVANL.....  147
136-142/L137         119  ................T.IVANL.....  147
143-147              119  ......................MK.P  147
L137E/143-147        119  ................E......MK.P  147
79-89/136-147        119  ................TEIVANL.MK.P  147
79-89/136-147/L137   119  ................T.IVANL.MK.P  147
```

Figure 2. Sequences of the human FcRn mutants (residues 79–147) analyzed here. Sequence identities (.) and differences (residues shown in bold) between wild-type human and mouse FcRn[13,26] are indicated. The double dash (– –) indicates a two residue deletion at positions 85 and 86 in human FcRn. The sequences of the generated mutants are shown, with identities (.) with human FcRn indicated. Sequences of these mutants outside residues 79–147 are the same as that of wild-type human FcRn.

the 143-147 mutant (with leucine at position 137) has dissociation constants that resemble those of wild-type human FcRn (Table 1). Of note, the non-conservative and helix-disrupting Asp (human) to Pro (mouse) change at position 147 (Figure 1 in the Supplementary Material; and Figure 1) therefore does not appear to affect the overall disposition of the binding surface. This was further substantiated by analyzing the combined effects of D147P plus L137E, which resulted in an FcRn species with properties analogous to those of L137E (data not shown). Thus, the positive effect of the 136-147 mutation cannot be fully recapitulated by mutating segments of amino acid residues, or individual residues, within this sequence.

Analyses of the effects of mutating residues 79–89 of human FcRn

Relative to mouse FcRn, the 136-147 mutant has reduced affinities for mouse IgG2b and human IgG1, and approximate four- to sixfold decreases in affinities are observed for the interaction of the 136-147/L137 mutant with mouse IgG1 (Table 1). These reduced affinities are most likely due to less favorable residue 137 (FcRn)–residue 436 (IgG) interactions (e.g. Glu137-Tyr436 or Leu137-His436; Table 1 of the Supplementary Material). However, and in contrast to the properties of the human FcRn (variants), unfavorable interactions between FcRn residue 137 and IgG residue 436 appear to be compensated for in the interactions of mouse FcRn

Table 1. Dissociation constants of the FcRn–IgG interactions

	Mouse IgG1		Mouse IgG2b		Human IgG1	
FcRn type	K_{D1} (μM)	K_{D2} (μM)	K_{D1} (μM)	K_{D2} (μM)	K_{D1} (μM)	K_{D2} (μM)
Wild-type human	WB[a]		8.3		0.37	2.1
Wild-type mouse	0.28	2.3	0.15	1.2	0.024	0.23
L137E[b]	13.2	ND[c]	11.7	ND	1.7	ND
136-147	0.34	3.0	0.69	6.0	0.20	6.4
136-147/L137	1.8	9.6	0.46	7.4	0.071	13.1
136-142	0.7	5.4	2.8	ND	0.28	1.7
136-142/L137	5.7	ND	0.57	4.5	0.1	4.4
143-147	WB		9.3	ND	0.18	2.9
L137E/143-147	15.2	ND	12.3	ND	0.69	11.3[d]
79-89/136-147[e]	**0.2**	**1.9**	**0.087**	**2.0**	**0.014**	**0.22**
79-89/136-147/L137	3.1	ND	0.092	1.3	0.021	0.23

[a] WB, very weak binding (K_D estimated to be >50 μM).
[b] Dissociation constants for this mutant are taken from our earlier study.[25]
[c] ND, not determined as data were adequately fit to a 1:1 interaction model.
[d] Fitting of the data for this interaction to a 1:1 model results in a estimate for K_{D1} of 1.6 μM.
[e] Shown in bold to indicate similarity with wild-type mouse FcRn.

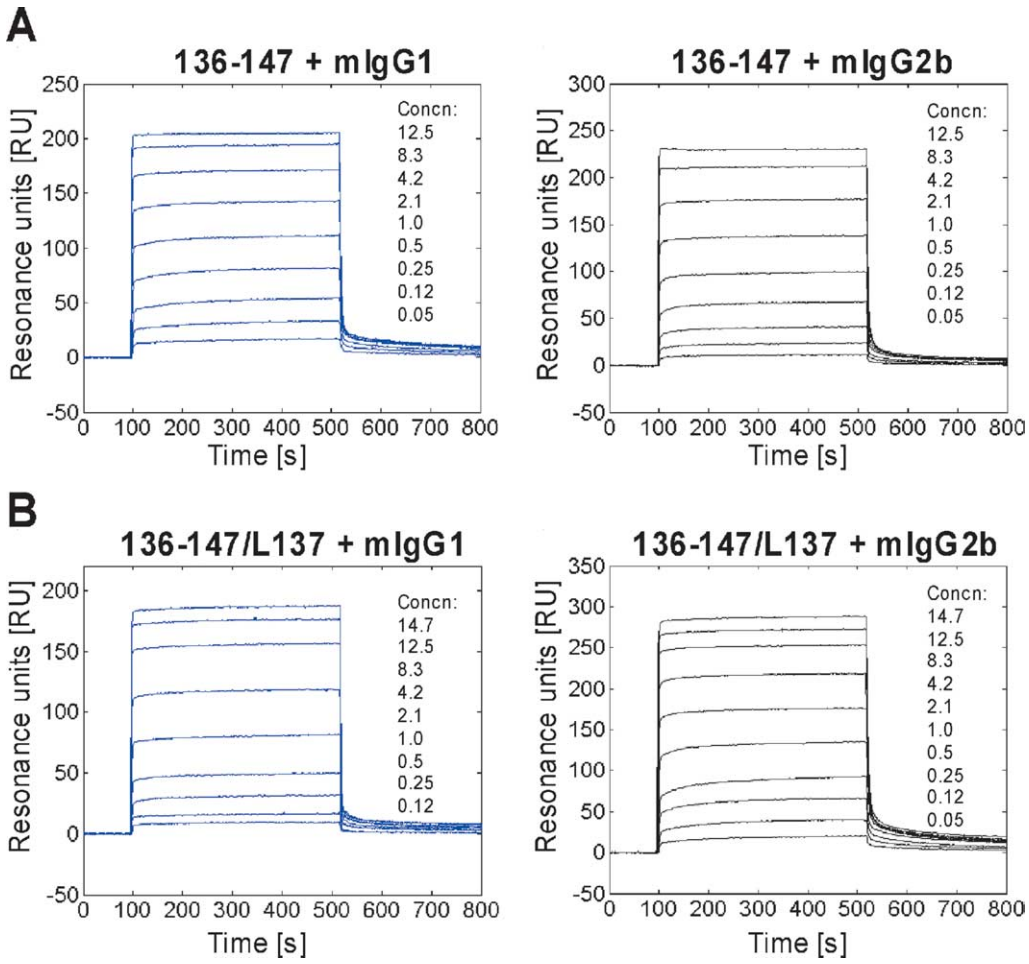

Figure 3. SPR analyses of the interactions of mouse IgG1 (mIgG1) and mouse IgG2b (mIgG2b) with (A) 136-147 mutant and (B) 136-147/L137 mutant. The coupling densities used were 480 RU (mouse IgG1) and 624 RU (mouse IgG2b). Different concentrations of FcRn mutants (0.05–14.7 μM) were injected over the flow cells in PBS (pH 6.0), 0.01% Tween at a flow rate of 10 μl/minute. Concentrations of FcRn mutants corresponding to each sensorgram are shown in μM. For all concentrations, duplicate injections were carried out and representative sensorgrams for each duplicate are shown. All sensorgrams were zero adjusted and reference cell data (flow cell coupled with buffer only during coupling cycle) subtracted.

with IgGs. For example, the dissociation constants of mouse FcRn for mouse IgG1 (His436) and mouse IgG2b (Tyr436) are in a similar range (work done by Zhou *et al*.[25] and Table 1). This prompted us to investigate other regions of FcRn that might be involved in modulating the residue 137 (FcRn)–436 (IgG) interaction.

Human FcRn has a deletion of residues 85 and 86, and the flanking residues (79–89) differ between mouse and human FcRn (Figure 1 of the Supplementary Material). In the X-ray crystallographic structure of rat FcRn bound to rat Fc (IgG2a), residues 86 (Ile in rat) and 90 (Phe in rat) contact Thr254 of IgG[21] (Figure 1). In an earlier study we noted that replacement of residues 79–89 of human FcRn by the corresponding mouse FcRn sequences in the presence or absence of the L137E mutation generated a human FcRn variant that bound to mouse IgG2b with the same affinity.[25] This observation suggested that this region in mouse FcRn could have longer-range effects on the interaction between FcRn residue 137 and IgG residue 436. We therefore combined the 79-89 mutation with 136-147 and 136-147/L137 mutations to generate 79-89/136-147 and 79-89/136-147/L137 mutants. The combination of the 79-89 and 136-147 mutations generates a human FcRn with properties very similar to those of mouse FcRn (Figure 5, Table 1). Notably, and as observed for mouse FcRn, the 79-89/136-147 mutant appears to be indifferent as to whether residue 436 of IgG is histidine or tyrosine (compare dissociation constants for mouse IgG1 *versus* mouse IgG2b). In contrast, relative to mouse FcRn, the 79-89/136-147/L137 mutant has an increased dissociation constant (K_{D1}; K_{D2} was too high to estimate under the conditions of the experiments) for interacting with mouse IgG1 whilst having similar properties for binding to mouse IgG2b and human IgG1 (Figure 5, Table 1). This suggests that interactions with the 79-89/136-147/L137 variant are more sensitive to incompatibilities of the 137 (FcRn)–436 (IgG) pair, and in

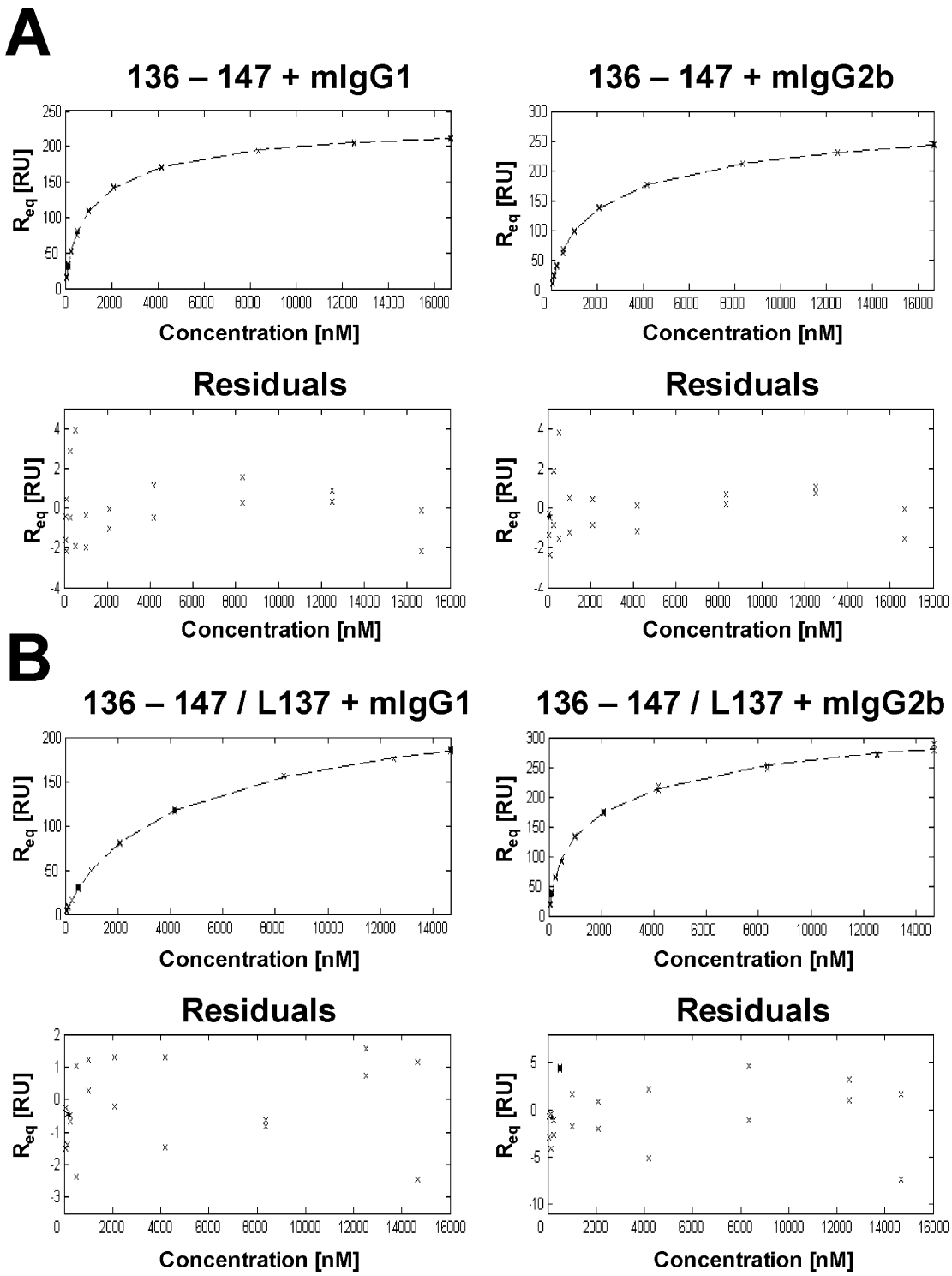

Figure 4. Analyses of the SPR data shown in Figure 3 using a model incorporating two non-equivalent binding sites on IgG and negative cooperativity. Data were fit as described in Methods. Analyte concentrations are shown in nM. The residuals are plotted below each fit.

this respect this mutant is similar to the related human FcRn mutant, 136-147/L137 (Table 1).

The pH dependence of the interactions

The interaction of mouse FcRn and wild-type human FcRn with IgGs is highly pH-dependent, with binding at pH 6.0 that becomes progressively weaker as pH 7.3 is approached.[22,23,25] We therefore analyzed whether the highest affinity mutants, 79-89/136-147 and 79-89/136-147/L137 had retained the pH dependence that is seen for the corresponding mouse FcRn interactions. Figure 6 shows that the 79-89/136-147 mutant, which at

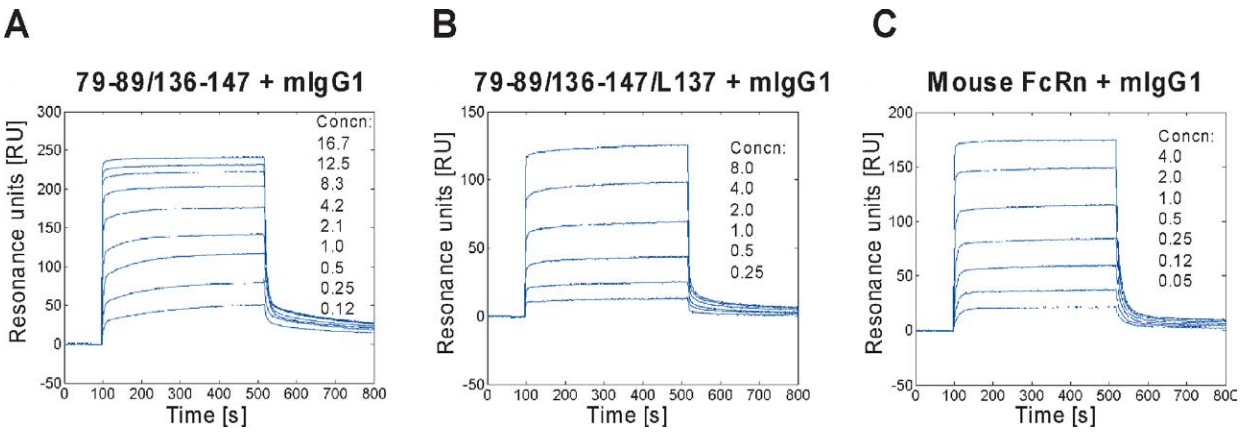

Figure 5. SPR analyses of the interactions of mouse IgG1 (mIgG1) with (A) 79-89/136-147 mutant, (B) 79-89/136-147/L137 mutant and (C) mouse FcRn. The coupling density of mouse IgG1 was 555 RU. Different concentrations of FcRn mutants (0.05–16.7 μM) were injected over the flow cells in PBS (pH 6.0), 0.01% Tween at a flow rate of 10 μl/minute. Concentrations of wild-type mouse FcRn or human FcRn mutants corresponding to each sensorgram are shown in μM. For all concentrations, duplicate injections were carried out and representative sensorgrams for each duplicate are shown. All sensorgrams were zero adjusted and reference cell data (flow cell coupled with buffer only during coupling cycle) subtracted.

pH 6.0 has binding properties that closely resemble those of mouse FcRn, binds to IgGs with markedly lower affinities at pH 7.3. The pH dependence of this mutant is very similar to that of mouse FcRn (Figure 6 and data not shown). In addition, as noted previously,[22,25] binding to mouse IgG1 (His436) shows more marked pH dependence than the interactions with mouse IgG2b or human IgG1 (both containing Tyr436). Although the 79-89/136-147/L137 mutant retains pH dependence for binding to mouse IgG1, less marked pH dependence is observed for the interactions of this mutant with human IgG1 and mouse IgG2b than for the 79-89/136-147 mutant (Figure 6 and data not shown).

Discussion

Here, we have used a combination of site-directed mutagenesis and SPR binding analyses to determine the molecular basis for the difference in binding specificity between mouse and human FcRn. By using iterative rounds of mutagenesis to confer the binding properties of mouse FcRn onto human FcRn in a stepwise fashion, we have identified two regions of FcRn that are functionally important. One of these regions encompasses and extends away from the key residue pair, FcRn residue 137 and IgG residue 436, whereas a second region in the α1 helix of FcRn appears to act as a modulator of the contribution of the residue 137 (FcRn)–436 (IgG) interaction. In contrast, sequence differences in the region encompassing residues 121-132 (Figure 1 of the Supplementary Material) that are in proximity to the FcRn–IgG interaction site[21] do not contribute to the difference in specificity between human and mouse FcRn (work done by Zhou *et al*.[25] and data not shown). Taken together, our studies lead to an improved understanding of the molecular details of FcRn–IgG interactions.

Structural and functional studies of FcRn and its IgG ligand indicate that residue 137 (Asp in rat FcRn, Glu in mouse FcRn and Leu in human FcRn) interacts with residue 436 (His in mouse IgG1, rat IgG2a and Tyr in mouse IgG2b, human IgG1) of IgG.[19,21] Loss of compatibility of this interacting pair has been suggested to be responsible for the inability of human FcRn to bind to mouse IgGs.[25] However, two observations indicate that there may be additional sequence variations between human and mouse FcRn that account for their marked differences in binding specificity. First, mouse FcRn binds to human IgG1 and mouse IgG2b with relatively high affinity, despite what might appear to be an unfavorable 137 (FcRn)–436 (IgG) pair (this study and the work done by Zhou *et al*.[25]). Second, mutation of Leu137 of human FcRn to Glu137 (L137E) generates a human FcRn variant that binds to mouse IgG1 and IgG2b, but with greatly reduced affinities compared with the corresponding mouse FcRn–mouse IgG interactions.[25] Here, we demonstrate that two additional regions of sequence can contribute to the functional differences across species.

By mutating sequences of the α2 helical region (residues 136–147) encompassing and extending away from the crucial residue 137 of human FcRn to those corresponding to mouse FcRn we have generated human FcRn variants with substantially improved affinities that approach those observed for the corresponding mouse FcRn–IgG interactions. Interestingly, this region contains a Pro (mouse FcRn) to Asp (human FcRn) difference at position 147, and we therefore analyzed whether the positive effect of mutating residues 136-147 could be recapitulated by alteration of a shorter segment (143–147) encompassing this residue in combination with the L137E mutation. This mutant

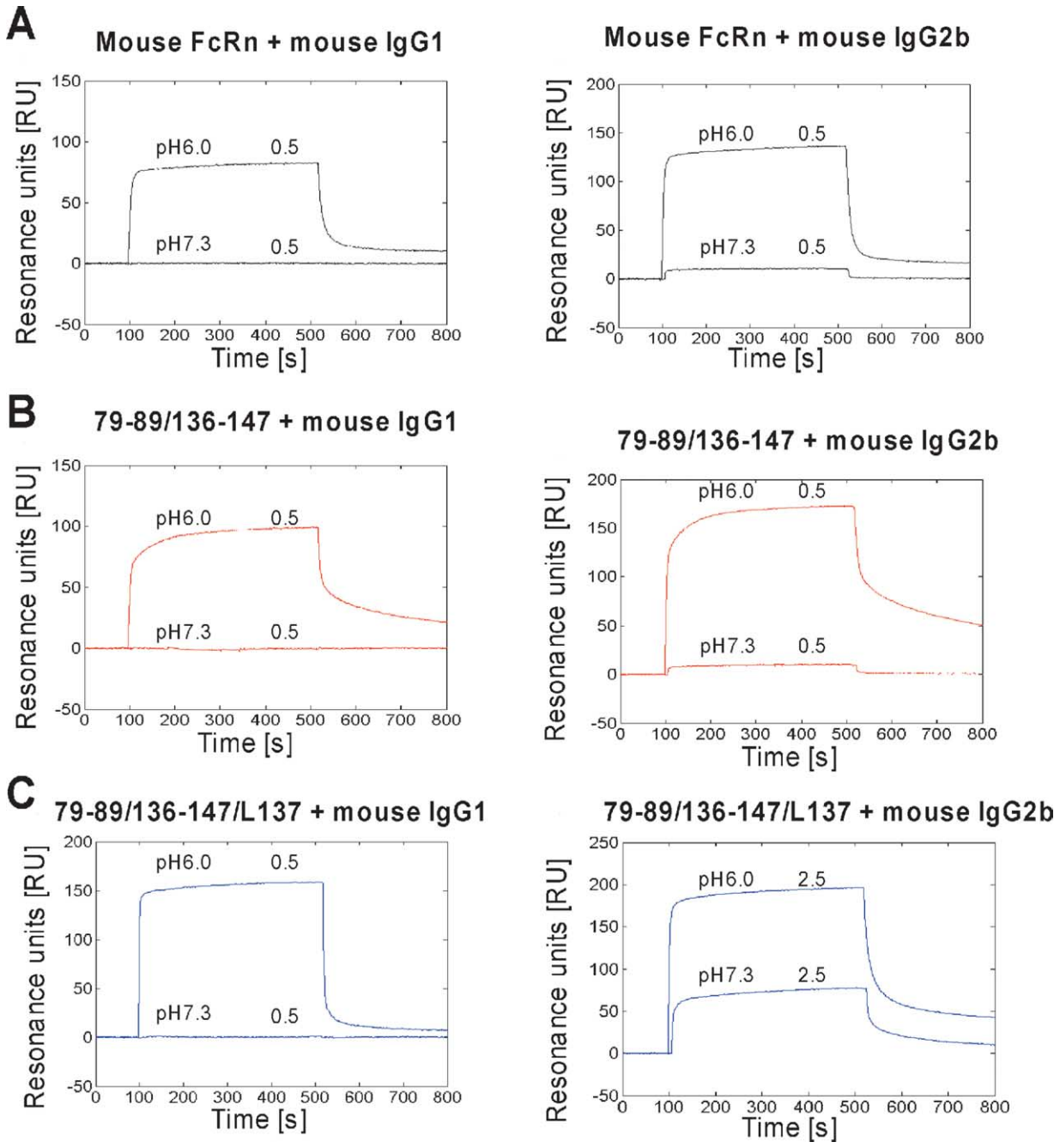

Figure 6. The pH dependence of the interactions of (A) mouse FcRn, (B) 79-89/136-147 mutant and (C) 79-89/136-147/L137 mutant with mouse IgG1 (mIgG1) and IgG2b (mIgG2b). The coupling densities of the IgGs were 555 RU (mouse IgG1 for A and B), 694 RU (mouse IgG1 for C) and 662 RU (mouse IgG2b for A, B and C). Sensorgrams for each FcRn species analyzed using PBS (pH 6.0 or pH 7.3 as indicated) plus 0.01% Tween as running buffer are shown, with pH and concentrations (0.5 μM or 2.5 μM) indicated. All sensorgrams are representative of duplicate injections and were zero adjusted and reference cell data (flow cell coupled with buffer only during coupling cycle) subtracted. Data for the pH dependence of binding of wild-type mouse FcRn and human FcRn variants to human IgG1 were similar to those shown for mouse IgG2b.

had essentially the same affinities for IgGs as those of the L137E mutation alone. This suggests that the effects of the 136–147 mutations may be due to differences in residues 136–142; however, mutation of residues 136–142 generated variants that in general had reduced affinities relative to the corresponding 136-147 mutants. Thus, at least from the mutations analyzed here, the positive effect of the 136-147 mutation cannot be fully attributed to subsets of residues within this sequence.

Despite the affinity improvements of the 136-147 (with Leu at 137) and 136-147 (with Glu at 137) mutants, these variants still retained a clear preference for Leu137–Tyr436 or Glu137–His436 interactions. For example, the 136-147 mutant has

similar dissociation constants for mouse IgG1 relative to those corresponding to mouse FcRn (Table 1), but decreased affinities for mouse IgG2b and human IgG1. This prompted us to analyze additional regions of sequence dissimilarity that might modulate the impact of the 137 (FcRn)–436 (IgG) pair. We therefore combined mutation of residues 79-89 of human FcRn with the 136-147 mutants (with Glu or Leu at position 137). The corresponding region of human FcRn has a two base-pair deletion (residues 85 and 86) and lacks the potential glycosylation site at position 87 that is present in rodent FcRn (Figure 1 of the Supplementary Material). Residues 86 and 90 of rat FcRn have been shown to contact IgG residue 254 in the X-ray structure of the corresponding complex.[21] Significantly, the effect of the 79-89 mutation, in combination with 136-147 (with Glu at 137) generates a human FcRn mutant that has properties similar to those of mouse FcRn. Perhaps unexpectedly, however, the 79-89 mutation plus 136-147/L137 (Leu at 137) mutation results in an increased dissociation constant for mouse IgG1 (Table 1). This suggests that although the 79-89 mutation can reduce the negative impact of an unfavorable Glu137-Tyr436 pair, this is not the case for the Leu137-His436 pair.

The molecular basis of the effects of the 79-89 mutation are currently not understood. However, as a consequence of the insertion of two amino acid residues, the α1 helix encompassing these residues is almost one turn longer than the corresponding region of human FcRn.[30] Mutation of human IgG1 residue 254 (Ser) to alanine results in a dramatic loss of affinity for binding to human FcRn,[18] suggesting that this residue might, by comparison with the rat FcRn–Fc structure,[21] contact human FcRn in the vicinity of residues 84, 87–90 (residues corresponding to 85 and 86 in rodent FcRn are absent in wild-type human FcRn) (Figure 1 of the Supplementary Material). Hence, it is possible that the shorter helix results in a slight reorientation of human FcRn on IgG relative to the rodent FcRn–IgG interactions, which might in turn affect the impact of the residue 137–residue 436 pair. In this context, the presence of additional carbohydrate at position 87 of FcRn is not predicted to play a role, as in rat FcRn this sugar does not contact Fc.[21] However, it is possible that carbohydrate at this position has more subtle steric effects on the overall topology of the interaction.

In general, the interaction of FcRn with homologous IgG is highly pH-dependent, with relatively high affinity binding at pH 6.0 that becomes progressively weaker as near neutral pH is approached.[22,31] This pH dependence is essential for functional activity,[32] as it is involved in the binding and release cycles that occur to transport IgG molecules within and across cells.[1,9] Analysis of the pH dependence of the two mutants that most closely resemble mouse FcRn (79-89/136-147/L137 and 79-89/136-147) indicates that pH dependencies analogous to those seen for mouse FcRn are only observed for the 79-89/136-147 mutant. Although the 79-89/136-147/L137 mutant binds to mouse IgG1 in a highly pH-dependent way, the pH dependence of the interactions with mouse IgG2b and human IgG1 (both with Tyr at residue 436) is reduced. This suggests that FcRn species with Glu137 (or Asp137) show greater pH dependence for binding to IgGs than those containing Leu137, even when the presumed partner residue on IgG is Tyr.

In summary, we have shown that it is possible to confer, by site-directed mutagenesis, the binding properties of mouse FcRn onto human FcRn. Residues in close proximity and more distal to the interaction site are responsible for the cross-species differences in specificity. The shorter α1 helix of human FcRn relative to that of rodent FcRn is also functionally relevant, as it appears to act as a modulator of key interactions. Thus, several regions of sequence variation appear to account for the marked differences in specificity between human and mouse FcRn. Our analyses extend the knowledge of human FcRn and its interactions with IgGs, and this has relevance to the use of antibodies in therapy.

Methods

Generation of plasmids for expression of mutated human FcRn

The plasmid DNA of human FcRn in pAcUW51[25] was used as a template for splicing by overlap extension[33] to generate the mutated variants of human FcRn shown in Figure 2. Mutated genes were subcloned as BglII-BamHI (sites which flank the mutated regions in the human FcRn gene[13]) fragments into pAcUW51 vector derivatives containing the human β_2-microglobulin gene[25] to generate the following mutants: 136-147, 136-147/L137, 136-142, 136-142/L137, 143-147, L137E/143-147, 79-89/136-147 and 79-89/136-147/L137 (Figure 2). To generate a mouse FcRn variant in which residues 136–147 were replaced by the corresponding human FcRn sequence, splicing by overlap extension[33] was used with the mouse FcRn gene in pAcUW51[23] as template. The mutated gene was recloned as a BamHI fragment into the BglII site of pAcUW51 containing the mouse β_2-microglobulin gene.[23] Sequences of mutagenic oligonucleotides are available on request. Clones harboring plasmid constructs with the desired orientation of the gene fragments were sequenced using an ABI PRISM model 3100.

Expression and purification of recombinant FcRn

Recombinant wild-type and mutated FcRn were expressed in insect cells (High-5; Invitrogen) infected with recombinant baculoviruses and protein was purified from culture supernatants using Ni^{2+}-NTA-agarose as described.[25] Aggregates were removed by subsequent purification using high-performance liquid chromatography and a HiLoad 26/60 Superdex™ 200 prep grade (Pharmacia) column.

Antibodies

Hulys10[34] and D1.3 (anti-lysozyme[35]) were used as a source of human and mouse IgG1 (both kappa),

respectively. Hulys10 is a humanized (human IgG1 constant region) antibody which recognizes hen egg lysozyme (HEL) and was purified from cell culture supernatants using HEL-Sepharose.[34] The HuLys10 cell line and D1.3 hybridoma were generous gifts from Dr Jeff Foote (Fred Hutchinson Cancer Center, Seattle) and Dr Roy Mariuzza (Center for Advanced Research in Biotechnology, Maryland), respectively. Mouse IgG2b was purchased from eBioscience.

Binding studies using surface plasmon resonance

SPR experiments were carried out using a BIAcore 2000. Flow cells of CM5 chips were coupled with human IgG1 (HuLys10), mouse IgG1 (D1.3) and mouse IgG2b using amine coupling chemistry. Reference flow cells were coupled with buffer only during the coupling cycle. For all of the FcRn species described in Figure 2, at least two analyses for each IgG were run with different batches of FcRn, different analyte concentration ranges, etc. Wild-type or mutated FcRn proteins were injected over the flow cells at a flow rate of 10 μl/minute at 25 °C. FcRn was injected at concentrations ranging from 0.05 μM to 16.7 μM. For all experiments, phosphate-buffered saline (PBS) pH 6.0 or pH 7.3 with 0.01% (v/v) Tween 20 and 0.02% (w/v) sodium azide was used as running buffer. For analyte injections carried out at pH 6.0, the same buffer at pH 7.2 was used to "strip" the flow cells at the end of each dissociation phase. Sensorgrams were zero adjusted, reference cell data subtracted and data analyzed using custom-written software†.

The equilibrium dissociation constants for interactions showing linear Scatchard plots were estimated using standard methods for a monophasic 1:1 interaction (e.g. as in Zhou *et al*.[25]). However, the majority of interactions resulted in biphasic Scatchards, consistent with studies showing that FcRn–IgG interactions involve two non-equivalent binding sites on IgG.[27,28] This is most likely due to steric effects of occupancy of the first binding site on IgG, which hinder binding to the second site.[29] These interactions were therefore fitted to a two-site model involving negative cooperativity using custom-written software. This generated estimates for two dissociation constants (K_{D1} and K_{D2}), which are taken to represent occupancy of the first site on IgG (K_{D1}) followed by binding to the second site with lower affinity (K_{D2}).

Acknowledgements

We are indebted to Jerry Chao and Palmer Long for excellent assistance with data analysis. This work was supported by grants from the National Institutes of Health (R01 AI 39167, RO1 GM 58538 and R01 AI 55556).

Supplementary Data

Supplementary data associated with this article can be found, in the online version, at doi:10.1016/j.jmb.2004.11.014

† http://www4.utsouthwestern.edu/wardlab/sprtool

References

1. Ghetie, V. & Ward, E. S. (2000). Multiple roles for the major histocompatibility complex class I-related receptor FcRn. *Annu. Rev. Immunol.* **18**, 739–766.
2. Praetor, A., Ellinger, I. & Hunziker, W. (1999). Intracellular traffic of the MHC class I-like IgG Fc receptor, FcRn, expressed in epithelial MDCK cells. *J. Cell Sci.* **112**, 2291–2299.
3. McCarthy, K. M., Yoong, Y. & Simister, N. E. (2000). Bidirectional transcytosis of IgG by the rat neonatal Fc receptor expressed in a rat kidney cell line: a system to study protein transport across epithelia. *J. Cell Sci.* **113**, 1277–1285.
4. Dickinson, B. L., Badizadegan, K., Wu, Z., Ahouse, J. C., Zhu, X., Simister, N. E. *et al*. (1999). Bidirectional FcRn-dependent IgG transport in a polarized human intestinal epithelial cell line. *J. Clin. Invest.* **104**, 903–911.
5. Claypool, S. M., Dickinson, B. L., Yoshida, M., Lencer, W. I. & Blumberg, R. S. (2002). Functional reconstitution of human FcRn in Madin-Darby canine kidney cells requires co-expressed human beta 2-microglobulin. *J. Biol. Chem.* **277**, 28038–28050.
6. Antohe, F., Radulescu, L., Gafencu, A., Ghetie, V. & Simionescu, M. (2001). Expression of functionally active FcRn and the differentiated bidirectional transport of IgG in human placental endothelial cells. *Hum. Immunol.* **62**, 93–105.
7. Kobayashi, N., Suzuki, Y., Tsuge, T., Okumura, K., Ra, C. & Tomino, Y. (2002). FcRn-mediated transcytosis of immunoglobulin G in human renal proximal tubular epithelial cells. *Am. J. Physiol. Renal Physiol.* **282**, F358–F365.
8. Ober, R. J., Martinez, C., Vaccaro, C., Zhou, J. & Ward, E. S. (2004). Visualizing the site and dynamics of IgG salvage by the MHC class I-related receptor, FcRn. *J. Immunol.* **172**, 2021–2029.
9. Ober, R. J., Martinez, C., Lai, X., Zhou, J. & Ward, E. S. (2004). Exocytosis of IgG as mediated by the receptor, FcRn: an analysis at the single-molecule level. *Proc. Natl Acad. Sci. USA*, **101**, 11076–11081.
10. Ghetie, V., Hubbard, J. G., Kim, J. K., Tsen, M. F., Lee, Y. & Ward, E. S. (1996). Abnormally short serum half-lives of IgG in beta 2-microglobulin-deficient mice. *Eur. J. Immunol.* **26**, 690–696.
11. Junghans, R. P. & Anderson, C. L. (1996). The protection receptor for IgG catabolism is the beta2-microglobulin-containing neonatal intestinal transport receptor. *Proc. Natl Acad. Sci. USA*, **93**, 5512–5516.
12. Israel, E. J., Wilsker, D. F., Hayes, K. C., Schoenfeld, D. & Simister, N. E. (1996). Increased clearance of IgG in mice that lack beta 2-microglobulin: possible protective role of FcRn. *Immunology*, **89**, 573–578.
13. Story, C. M., Mikulska, J. E. & Simister, N. E. (1994). A major histocompatibility complex class I-like Fc receptor cloned from human placenta: possible role in transfer of immunoglobulin G from mother to fetus. *J. Expt. Med.* **180**, 2377–2381.
14. Ober, R. J., Radu, C. G., Ghetie, V. & Ward, E. S. (2001). Differences in promiscuity for antibody-FcRn interactions across species: implications for therapeutic antibodies. *Int. Immunol.* **13**, 1551–1559.
15. Kim, J. K., Tsen, M. F., Ghetie, V. & Ward, E. S. (1994). Localization of the site of the murine IgG1 molecule that is involved in binding to the murine intestinal Fc receptor. *Eur. J. Immunol.* **24**, 2429–2434.
16. Medesan, C., Matesoi, D., Radu, C., Ghetie, V. & Ward,

E. S. (1997). Delineation of the amino acid residues involved in transcytosis and catabolism of mouse IgG1. *J. Immunol.* **158**, 2211–2217.
17. Kim, J. K., Firan, M., Radu, C. G., Kim, C. H., Ghetie, V. & Ward, E. S. (1999). Mapping the site on human IgG for binding of the MHC class I-related receptor, FcRn. *Eur. J. Immunol.* **29**, 2819–2825.
18. Shields, R. L., Namenuk, A. K., Hong, K., Meng, Y. G., Rae, J., Briggs, J. *et al*. (2001). High resolution mapping of the binding site on human IgG1 for Fc gamma RI, Fc gamma RII, Fc gamma RIII, and FcRn and design of IgG1 variants with improved binding to the Fc gamma R. *J. Biol. Chem.* **276**, 6591–6604.
19. Vaughn, D. E., Milburn, C. M., Penny, D. M., Martin, W. L., Johnson, J. L. & Bjorkman, P. J. (1997). Identification of critical IgG binding epitopes on the neonatal Fc receptor. *J. Mol. Biol.* **274**, 597–607.
20. Burmeister, W. P., Huber, A. H. & Bjorkman, P. J. (1994). Crystal structure of the complex of rat neonatal Fc receptor with Fc. *Nature*, **372**, 379–383.
21. Martin, W. L., West, A. P. J., Gan, L. & Bjorkman, P. J. (2001). Crystal structure at 2.8 Å of an FcRn/heterodimeric Fc complex: mechanism of pH dependent binding. *Mol. Cell*, **7**, 867–877.
22. Raghavan, M., Bonagura, V. R., Morrison, S. L. & Bjorkman, P. J. (1995). Analysis of the pH dependence of the neonatal Fc receptor/immunoglobulin G interaction using antibody and receptor variants. *Biochemistry*, **34**, 14649–14657.
23. Popov, S., Hubbard, J. G., Kim, J., Ober, B., Ghetie, V. & Ward, E. S. (1996). The stoichiometry and affinity of the interaction of murine Fc fragments with the MHC class I-related receptor, FcRn. *Mol. Immunol.* **33**, 521–530.
24. Simister, N. E. & Mostov, K. E. (1989). An Fc receptor structurally related to MHC class I antigens. *Nature*, **337**, 184–187.
25. Zhou, J., Johnson, J. E., Ghetie, V., Ober, R. J. & Ward, E. S. (2003). Generation of mutated variants of the human form of the MHC class I-related receptor, FcRn, with increased affinity for mouse immunoglobulin G. *J. Mol. Biol.* **332**, 901–913.
26. Ahouse, J. J., Hagerman, C. L., Mittal, P., Gilbert, D. J., Copeland, N. G., Jenkins, N. A. & Simister, N. E. (1993). Mouse MHC class I-like Fc receptor encoded outside the MHC. *J. Immunol.* **151**, 6076–6088.
27. Schuck, P., Radu, C. G. & Ward, E. S. (1999). Sedimentation equilibrium analysis of recombinant mouse FcRn with murine IgG1. *Mol. Immunol.* **36**, 1117–1125.
28. Sanchez, L. M., Penny, D. M. & Bjorkman, P. J. (1999). Stoichiometry of the interaction between the major histocompatibility complex-related Fc receptor and its Fc ligand. *Biochemistry*, **38**, 9471–9476.
29. Weng, Z., Gulukota, K., Vaughn, D. E., Bjorkman, P. J. & DeLisi, C. (1998). Computational determination of the structure of rat Fc bound to the neonatal Fc receptor. *J. Mol. Biol.* **282**, 217–225.
30. West, A. P. J. & Bjorkman, P. J. (2000). Crystal structure and immunoglobulin G binding properties of the human major histocompatibility complex-related Fc receptor. *Biochemistry*, **39**, 9698–9708.
31. Roberts, D. M., Guenthert, M. & Rodewald, R. (1990). Isolation and characterization of the Fc receptor from the fetal yolk sac of the rat. *J. Cell Biol.* **111**, 1867–1876.
32. Dall'Acqua, W., Woods, R. M., Ward, E. S., Palaszynski, S. R., Patel, N. K., Brewah, Y. A. *et al*. (2002). Increasing the affinity of a human IgG1 to the neonatal Fc receptor: biological consequences. *J. Immunol.* **169**, 5171–5180.
33. Horton, R. M., Hunt, H. D., Ho, S. N., Pullen, J. K. & Pease, L. R. (1989). Engineering hybrid genes without the use of restriction enzymes: gene splicing by overlap extension. *Gene*, **77**, 61–68.
34. Foote, J. & Winter, G. (1992). Antibody framework residues affecting the conformation of the hypervariable loops. *J. Mol. Biol.* **224**, 487–499.
35. Amit, A. G., Mariuzza, R. A., Phillips, S. E. & Poljak, R. J. (1986). Three-dimensional structure of an antigen-antibody complex at 2.8 Å resolution. *Science*, **233**, 747–753.

Edited by I. Wilson

(Received 23 July 2004; received in revised form 1 November 2004; accepted 7 November 2004)